Cylindrical Coordinate Control of Three-Dimensional PWM Technique in Three-Phase Four-Wired Trilevel Inverter

Man-Chung Wong, Jing Tang, *Student Member, IEEE,* and Ying-Duo Han

***Abstract*—In past decades, almost all the studies are focused in two-dimensional (2-D) PWM techniques on α–β frame. Recently, four-legs inverter is proposed to compensate the three-phase four-wired system issues. However, three-legs center-split inverter can be applied to compensate the power quality issues including the zero-sequence compensation by the novel PWM technique: three-dimensional (3-D) PWM. In this paper, the mathematical model of shunt-connected three-level power inverter in three-phase four-wired system is studied in a–b–c–0 frame. The study of 3-D voltage space vector PWM technique in two-level and three-level inverters is performed in rectangular, cylindrical, and spherical coordinates, respectively. The 3DPWM performance indices are proposed. Comparative study of fixed switching sign cubical hysteresis control with this novel proposed technique "cylindrical coordinate control strategy" is accomplished. The results show that the performance of the proposed novel control strategy can overcome the drawbacks of fixed switching sign cubical hysteresis 3DPWM control strategy.**

***Index Terms*—3DPWM, three-phase four-wired system, multilevel inverter, power quality.**

I. Introduction

FOR THE high voltage power applications, the multi-level VSI topologies are good alternatives. The multi-level structure not only reduces voltage stress across the switches but also provides many more available vectors. Therefore, it improves harmonic contents of the VSI by selecting appropriate switching vectors. The most popular topology is the three-level inverter. Up to now, many studies have been presented on PWM strategies for three-level inverters including carrier-based sub-oscillation methods [1], [2], harmonics elimination techniques [3], [4], optimal strategies [4], [5], dipolar modulation [6] and space vector PWM [7]. While the multilevel PWM techniques are developed, the two-level PWM methods are extended into multi-level one, such as carrier-based and carrier-less PWM techniques [4]–[7]. The multilevels of these inverters offer more degrees of freedom in choosing vectors and with greater possibilities in terms of device utilization, state redundancies and effectively reducing the switching-frequency. However, in past decades, almost all the PWM researches [8]–[10] are focused in the two-dimensional (2-D) PWM techniques, no matter they are two-level or multilevel systems. The reason may be that the three-phase three-wired inverters are the main focus for the PWM researches in past decades.

Due to the development of the "custom power" concept, three-phase four-wired system will play a very important role in the distribution site. On the other hand, some researches pointed out the four-leg converter topology as the best means to implement a three-phase four-wired inverter system [11], [12]. Although three-phase four-wired active filters have been introduced in 1980s [11], the development is still at its infancy. The development of instantaneous reactive power theory [13] is begun in 1984 for instantaneous three-phase compensation in α–β frame. Until 1998, a generalized theory of instantaneous reactive power [14] was proposed and developed. This generalized instantaneous reactive power theory is valid for sinusoidal or nonsinusoidal and balanced or unbalanced three-phase systems, with or without zero-sequence currents and/or voltages. It gives concise theory background to compensate harmonics, reactive power and unbalance in three-phase four-wired system for power quality compensators. In 2000, three-dimensional (3-D) vector control strategy [12] was proposed, but it worked for four-legs inverter systems. The three-legs "split-capacitor" inverters are reported to compensate the zero-sequence current in [11]. Unfortunately, it [11] reported and compared to the power control strategies only, it did not inform the PWM technique's characteristics in three-phase four-wired inverter.

In 2001, the mathematical model of 3-D PWM technique [15] is proposed for "center-split" three-legs inverter and extended into three-level inverters for three-phase four-wired system. In conventional PWM techniques, the number of states for two-level and three-level inverters is seven and 19, respectively, although there are eight and 27 available vectors totally. However, in 3-D PWM techniques the number of states in two-level and three-level inverters is the same as the number of available vectors. The explanation will be addressed in Section II-B. The compensated performance of 3-DPWM is already achieved and tested by sign cubical hysteresis control strategy [15]. The main drawbacks of the sign cubical hysteresis control strategy are as follows.

1) The special vectors [15] divert one improvement in one direction and will give dedicated error in another direction.

2) Switching frequency is relatively high and random.

Manuscript received February 28, 2002; revised September 10, 2002. This work was supported by the Ph.D. Fund, Chinese Education Ministry and Research Fund, Research Committee, University of Macau. Recommended by Associate Editor F. Blaabjerg.

M.-C. Wong is with the Faculty of Science and Technology, University of Macau, China. He is also with Tsinghua University, China (e-mail: mcwong@umac.mo).

J. Tang is with the Faculty of Science and Technology, University of Macau, China.

Y.-D. Han is with the Department of Electrical Engineering, Tsinghua University, China. He is also with the University of Macau, China.

Digital Object Identifier 10.1109/TPEL.2002.807133

3) The compensated results may be unstable due to the over-compensation or under-compensation when the switching frequency is fixed and the results are easy to be affected by the system's parameters.

In this paper, the novel cylindrical coordinate control 3DPWM is proposed for reducing the switching frequency and eliminating special vectors effects. The corresponding voltage value [16] can be determined according to the required current signals and is modified in Section III-A. There are already many researches that discussed about the neutral-point potential control [5], [17] for three-level inverters. The neutral-point potential control is not discussed in this paper. The focus will be on the analysis of 3DPWM voltage space vectors and the improvement of 3DPWM control strategy in three-level inverters. Novel performance indices are proposed for 3-D PWM study and comparison between fixed sign cubical hysteresis control strategy [15] and this novel cylindrical coordinate control of 3DPWM is achieved.

II. Basic Principles

A. Modeling of Trilevel Three-Phase Four-Wired Converter

The physical model of shunt three-phase four-wired three-level converter, as shown in Fig. 1, is investigated in the a–b–c–0 frame. The loss of the switching devices, snubber circuits, and process of commutation are ignored so that the equivalent switched-circuit can be obtained in Fig. 2.

In the equivalent circuit model shown in Fig. 2, the switching function can be expressed for switching device, IGBT. For example, in phase a, switching function S_a can be written as

$$S_a = \begin{cases} 1, & \text{when } T_{1a} \text{ and } T_{2a} \text{ are closed } (S_{1a}) \\ 0, & \text{when } T_{2a} \text{ and } T_{3a} \text{ are closed } (S_{3a}) \\ -1, & \text{when } T_{3a} \text{ and } T_{4a} \text{ are closed } (S_{2a}). \end{cases} \tag{1}$$

There are three cases in one arm of the three-level converters: positive, zero and negative switching functions.

1) if $S_a = 1$, then $S_{1a} = 1$, $S_{2a} = 0$, $S_{3a} = 0$.
2) if $S_a = 0$, then $S_{1a} = 0$, $S_{2a} = 0$, $S_{3a} = 1$.
3) if $S_a = -1$, then $S_{1a} = 0$, $S_{2a} = 1$, $S_{3a} = 0$.

It is noticed that S_a, S_b and S_c can be 1, 0 and -1. In Fig. 2, the boundary condition of S_{1a}, S_{2a} and S_{3a} is defined as

$$\begin{cases} S_{1a} + S_{2a} + S_{3a} = 1 \\ S_{1a} = 1 \text{ or } 0, \quad S_{2a} = 1 \text{ or } 0, \quad S_{3a} = 1 \text{ or } 0. \end{cases} \tag{2}$$

It means that when S_{1a} is equal to 1 then S_{2a} and S_{3a} must be zero: $S_a \in \{-1, 0, 1\}$. However, the neutral (zero) voltage and neutral (zero) current can be defined as (3) and (4), respectively

$$v_N = \tfrac{1}{3}(v_a + v_b + v_c) \tag{3}$$

$$i_N = \tfrac{1}{3}(i_a + i_b + i_c). \tag{4}$$

According to the equations (3), (4), and Fig. 2, the relation among the ac-side compensating current (i_{ca}, i_{cb}, i_{cc}, i_{cN}), the coupling terminal voltage (v_{sa}, v_{sb}, v_{sc}, v_{sN}) and the terminal voltage (v_a, v_b, v_c, v_N) of the inverter can be expressed as

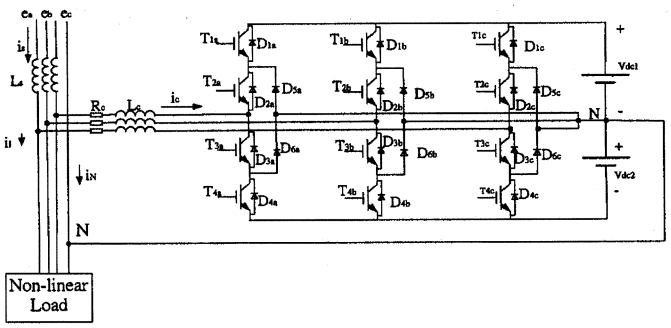

Fig. 1. Three-phase four-wired three-level converter.

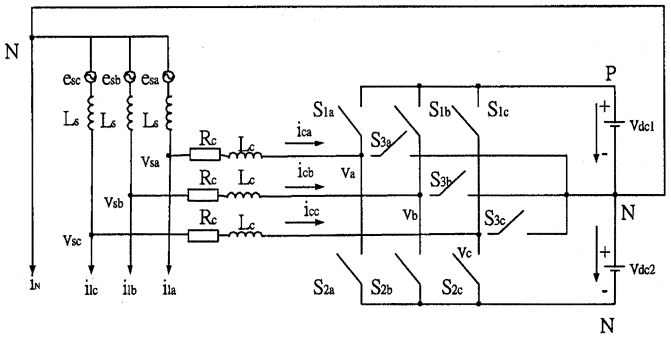

Fig. 2. Equivalent model of three-phase four-wired trilevel converter.

$$\begin{cases} L_c \dfrac{di_{ca}}{dt} = -R_c \cdot i_{ca} - v_a + v_{sa} \\ L_c \dfrac{di_{cb}}{dt} = -R_c \cdot i_{cb} - v_b + v_{sb} \\ L_c \dfrac{di_{cc}}{dt} = -R_c \cdot i_{cc} - v_c + v_{sc} \\ L_c \dfrac{di_{cN}}{dt} = -R_c \cdot i_{cN} - v_N + v_{sN}. \end{cases} \tag{5}$$

By the switching functions, the relation between the terminal voltage (v_a, v_b, v_c) and the dc-link voltage (v_{dc1}, v_{dc2}) of the inverters can be expressed as

$$\begin{cases} v_a = S_{1a} \cdot v_{dc1} - S_{2a} \cdot v_{dc2} \\ v_b = S_{1b} \cdot v_{dc1} - S_{2b} \cdot v_{dc2} \\ v_c = S_{1c} \cdot v_{dc1} - S_{2c} \cdot v_{dc2}. \end{cases} \tag{6}$$

A general mathematical model of the Tri-level Converter in a–b–c–0 frame can be established as

$$\boldsymbol{Z}\dot{\boldsymbol{X}} = \boldsymbol{A}\boldsymbol{X} + \boldsymbol{B}\boldsymbol{U} \tag{7}$$

where as shown in the equation at the bottom of the next page.

B. Three Dimensional Pulse-Width Modulation Technique

In three-phase three-wired system, there are many researches focusing on the pulse-width modulation techniques such as the sinusoidal PWM, hysteresis control PWM, and space vector PWM etc. However, all of them are only investigated in 2-D aspect. Only 2-D PWM cannot be utilized to solve the issues

in three-phase four-wired system. In conventional PWM techniques, the number of states is not equal to the number of available vectors. The mathematical model of 3-D pulse-width modulation is described in this section. Voltage vector allocation is also discussed with respect to the conventional 2DPWM and this novel 3DPWM.

It is assumed that the upper-arm and the lower-arm battery voltages are the same: $V_{dc1} = V_{dc2} = V_{dc}$. According to the concept of switching functions and α–β–0 frame transformation, the instantaneous voltage vector is given as

$$\vec{v} = V_{dc}\left[\sqrt{\frac{2}{3}}\,S_\alpha \cdot \vec{n}_\alpha + \frac{1}{\sqrt{2}}\,S_\beta \cdot \vec{n}_\beta + \frac{1}{\sqrt{3}}\,S_0 \cdot \vec{n}_0\right] \quad (8)$$

where

$$\begin{aligned} S_\alpha &= S_a - \tfrac{1}{2}\,S_b - \tfrac{1}{2}\,S_c \\ S_\beta &= S_b - S_c \\ S_0 &= S_a + S_b + S_c. \end{aligned}$$

In 3-D aspect, PWM can be expressed in rectangular, cylindrical or spherical coordinates. In the rectangular coordinate, $\{\vec{n}_\alpha, \vec{n}_\beta, \vec{n}_0\}$ form a basis and they are orthogonal to each other such that $\vec{n}_0 \bullet \vec{n}_\alpha = \vec{n}_0 \bullet \vec{n}_\beta = \vec{n}_\alpha \bullet \vec{n}_\beta = 0$. The instantaneous voltage vector can also be expressed as

$$\begin{aligned} \vec{v} = v_\alpha \vec{n}_\alpha + v_\beta \vec{n}_\beta + v_0 \vec{n}_0, \quad \text{where } v_\alpha = V_{dc} \cdot Z_\alpha, \\ v_\beta = V_{dc} \cdot Z_\beta \quad \text{and} \quad v_0 = V_{dc} \cdot Z_0. \end{aligned} \quad (9)$$

The parameters describing the rectangular coordinate are Z_α, Z_β, Z_0 and the distance ρ shown in (10) is the actual vector's amplitude

$$\begin{aligned} \rho = \sqrt{Z_\alpha^2 + Z_\beta^2 + Z_0^2} \quad \text{where } Z_\alpha = \sqrt{\frac{2}{3}}\,S_\alpha, \\ Z_\beta = \frac{1}{\sqrt{2}}\,S_\beta, \quad Z_0 = \frac{1}{\sqrt{3}}\,S_0. \end{aligned} \quad (10)$$

In cylindrical coordinate, each point P in space receives the name $\{r, \theta, Z_0\}$ as shown in Fig. 3. On the other hand, $\{\rho, \theta, \phi\}$ can be used to describe a point P in Spherical Coordinate (Fig. 4). "r" and "θ" are the polar distance and angle respectively in α–β frame

$$r = \sqrt{Z_\alpha^2 + Z_\beta^2} \quad (11)$$

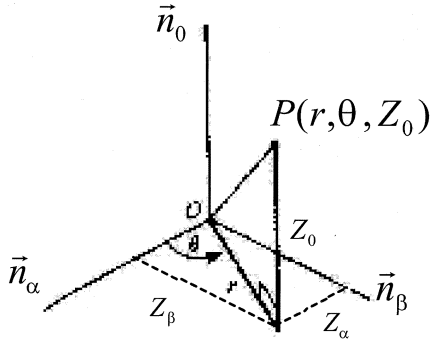

Fig. 3. Cylindrical coordinate.

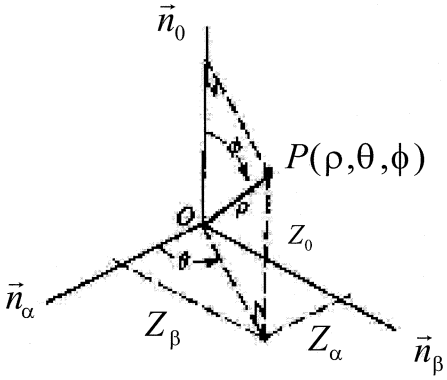

Fig. 4. Spherical coordinate.

$$\theta = \tan^{-1}\left(\frac{Z_\beta}{Z_\alpha}\right) \quad (12)$$

$$\phi = \cos^{-1}\left(\frac{Z_0}{\rho}\right) = \sin^{-1}\left(\frac{r}{\rho}\right). \quad (13)$$

1) Two-Level 3DPWM System: In the two-level conventional pulse width modulation techniques, the voltage space vectors can be illustrated in α–β frame, shown in Fig. 5. The number of states in two-level system is seven although there are eight available vectors altogether. There are totally eight voltage vectors with six directional vectors and two zero vectors. However, in past researches, these two zero vectors were utilized in optimizing the switching losses. But, in 3DPWM, these two vectors dedicated as the zero-axis voltage components in positive and negative directions respectively. Table I

$$\mathbf{A} = \begin{bmatrix} -R_c & 0 & 0 & 0 & -S_{1a} & S_{2a} \\ 0 & -R_c & 0 & 0 & -S_{1b} & S_{2b} \\ 0 & 0 & -R_c & 0 & -S_{1c} & S_{2c} \\ 0 & 0 & 0 & -R_c & -\left(\dfrac{S_{1a}+S_{1b}+S_{1c}}{3}\right) & \left(\dfrac{S_{2a}+S_{2b}+S_{2c}}{3}\right) \end{bmatrix}$$

$$\mathbf{X} = [\,i_{ca} \quad i_{cb} \quad i_{cc} \quad i_{cN} \quad V_{dc1} \quad V_{dc2}\,]^T$$

$$\mathbf{B} = \mathrm{diag}[\,1 \quad 1 \quad 1 \quad 1\,]$$

$$\mathbf{U} = [\,v_{sa} \quad v_{sb} \quad v_{sc} \quad v_{sN}\,]$$

$$\mathbf{Z} = \mathrm{diag}[\,L_c \quad L_c \quad L_c \quad L_c\,].$$

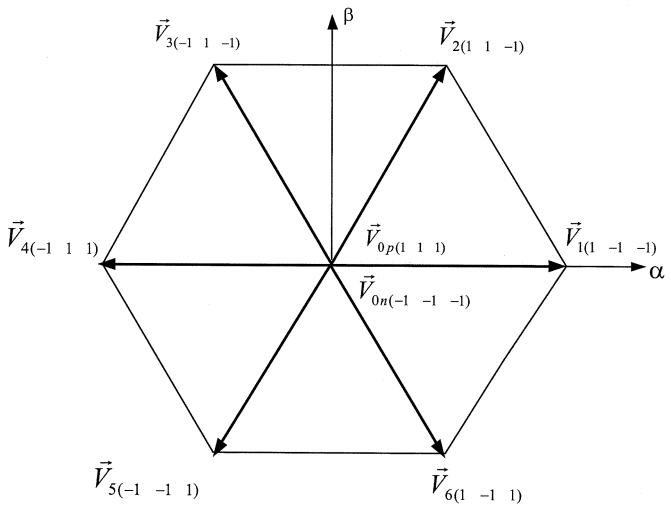

Fig. 5. Two-level voltage space vector's allocation in $\alpha-\beta$ frame.

TABLE I
TWO-LEVEL 3DPWM VOLTAGE VECTOR'S PARAMETERS

	S_a	S_b	S_c	S_α	S_β	S_0	r	θ	Z_0	ρ	ϕ
$\vec{V}_1$	1	-1	-1	2	0	-1	1.633	0^0	-0.577	$\sqrt{3}$	109.46^0
$\vec{V}_2$	1	1	-1	1	2	1	1.633	60^0	0.577	$\sqrt{3}$	70.54^0
$\vec{V}_3$	-1	1	-1	-1	2	-1	1.633	120^0	-0.577	$\sqrt{3}$	109.46^0
$\vec{V}_4$	-1	1	1	-2	0	1	1.633	180^0	0.577	$\sqrt{3}$	70.54^0
$\vec{V}_5$	-1	-1	1	-1	-2	-1	1.633	240^0	-0.577	$\sqrt{3}$	109.46^0
$\vec{V}_6$	1	-1	1	1	-2	1	1.633	300^0	0.577	$\sqrt{3}$	70.54^0
$\vec{V}_{00p}$	1	1	1	0	0	3	0	*	$\sqrt{3}$	$\sqrt{3}$	0^0
$\vec{V}_{00n}$	-1	-1	-1	0	0	-3	0	*	$-\sqrt{3}$	$\sqrt{3}$	180^0

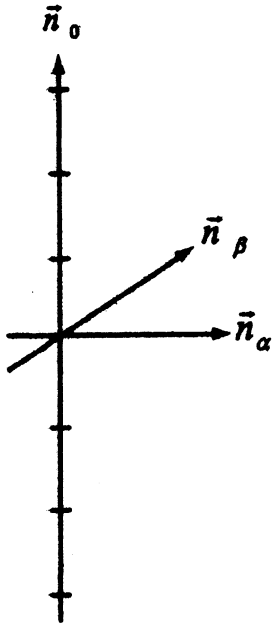

Fig. 6. Basis $\{\vec{n}_\alpha, \vec{n}_\beta, \vec{n}_0\}$.

summarized the parameters describing the 3DPWM voltage vectors in rectangular, cylindrical, and spherical coordinates. The mark "$*$" means "undefined" in the following Tables.

The two-level voltage vector's allocation is better to be described in 3-D aspect. Fig. 6 shows the basis $\{\vec{n}_\alpha, \vec{n}_\beta, \vec{n}_0\}$ and

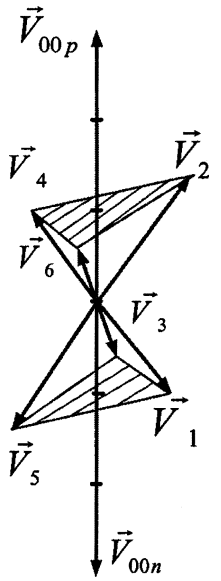

Fig. 7. Two-level 3-D voltage vectors.

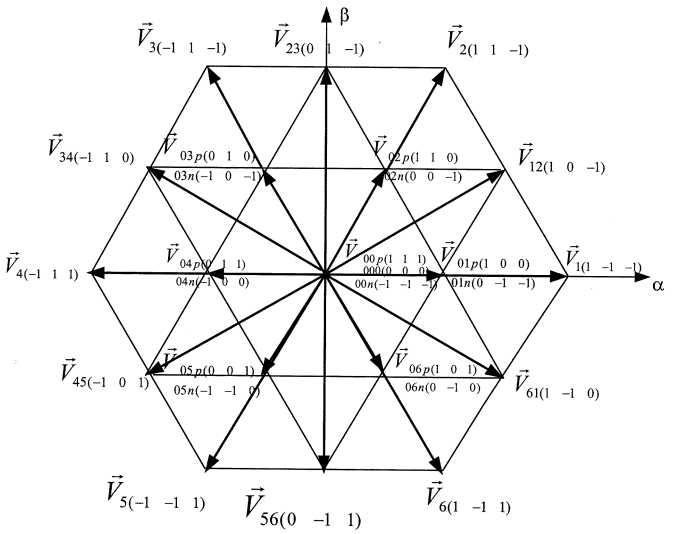

Fig. 8. Three-level voltage vector's allocation.

Fig. 7 represents the actual voltage vector's allocation. It is clear that the conventional 2-D PWM voltage vector's allocation is just the top view of 3DPWM. Actually, 2-D PWM technique is a subset of 3-D PWM. The vectors $\{\vec{V}_2, \vec{V}_4, \vec{V}_6\}$ and $\{\vec{V}_1, \vec{V}_3, \vec{V}_5\}$ lie on the different horizontal planes shown in Fig. 7.

2) Three-Level 3DPWM System: A typical case of multilevel converters is a trilevel one. In this section, 3-D PWM is studied in three-level system aspect. The number of vectors, which can be implemented in the three-level VSI, is 27. These can be categorized into four different vectors: large-, mid-, small-, and zero-vectors. The conventional picture describing the three-level voltage vector's allocation is shown in Fig. 8. There is a larger degree of freedom in choosing vectors in three-level case according to the compensating requirement. The conventional three-level PWM techniques have 19 states and 27 available vectors. The number of states is not equal to the number of vectors. However, in 3DPWM, the number of states can be equal to the number of available vectors.

TABLE II
ZERO VECTORS

	S_a	S_b	S_c	S_α	S_β	S_0	r	θ	Z_0	ρ	ϕ
$\vec{V}_{000}$	0	0	0	0	0	0	0	*	0	0	*
$\vec{V}_{00\,p}$	1	1	1	0	0	3	0	*	$\sqrt{3}$	$\sqrt{3}$	0^0
$\vec{V}_{00\,n}$	-1	-1	-1	0	0	-3	0	*	$-\sqrt{3}$	$\sqrt{3}$	180^0

TABLE III
SMALL VECTORS

	S_a	S_b	S_c	S_α	S_β	S_0	r	θ	Z_0	ρ	ϕ
$\vec{V}_{01\,p}$	1	0	0	1	0	1	0.816	0^0	0.577	1	54.76^0
$\vec{V}_{01\,n}$	0	-1	-1	1	0	-2	0.816	0^0	-1.155	$\sqrt{2}$	144.76^0
$\vec{V}_{02\,p}$	1	1	0	0.5	1	2	0.816	60^0	1.155	$\sqrt{2}$	35.24^0
$\vec{V}_{02\,n}$	0	0	-1	0.5	1	-1	0.816	60^0	-0.577	1	125.24^0
$\vec{V}_{03\,p}$	0	1	0	-0.5	1	1	0.816	120^0	0.577	1	54.76^0
$\vec{V}_{03\,n}$	-1	0	-1	-0.5	1	-2	0.816	120^0	-1.155	$\sqrt{2}$	144.76^0
$\vec{V}_{04\,p}$	0	1	1	-1	0	2	0.816	180^0	1.155	$\sqrt{2}$	35.24^0
$\vec{V}_{04\,n}$	-1	0	0	-1	0	-1	0.816	180^0	-0.577	1	125.24^0
$\vec{V}_{05\,p}$	0	0	1	-0.5	-1	1	0.816	240^0	0.577	1	54.76^0
$\vec{V}_{05\,n}$	-1	-1	0	-0.5	-1	-2	0.816	240^0	-1.155	$\sqrt{2}$	144.76^0
$\vec{V}_{06\,p}$	1	0	1	0.5	-1	2	0.816	300^0	1.155	$\sqrt{2}$	35.24^0
$\vec{V}_{06\,n}$	0	-1	0	0.5	-1	-1	0.816	300^0	-0.577	1	125.24^0

TABLE IV
MEDIUM VECTORS

	S_a	S_b	S_c	S_α	S_β	S_0	r	θ	Z_0	ρ	ϕ
$\vec{V}_{12}$	1	0	-1	1.5	1	0	$\sqrt{2}$	30^0	0	$\sqrt{2}$	90^0
$\vec{V}_{23}$	0	1	-1	0	2	0	$\sqrt{2}$	90^0	0	$\sqrt{2}$	90^0
$\vec{V}_{34}$	-1	1	0	-1.5	1	0	$\sqrt{2}$	150^0	0	$\sqrt{2}$	90^0
$\vec{V}_{45}$	-1	0	1	-1.5	-1	0	$\sqrt{2}$	210^0	0	$\sqrt{2}$	90^0
$\vec{V}_{56}$	0	-1	1	0	-2	0	$\sqrt{2}$	270^0	0	$\sqrt{2}$	90^0
$\vec{V}_{61}$	1	-1	0	1.5	-1	0	$\sqrt{2}$	330^0	0	$\sqrt{2}$	90^0

TABLE V
LARGE VECTORS

	S_a	S_b	S_c	S_α	S_β	S_0	r	θ	Z_0	ρ	ϕ
$\vec{V}_1$	1	-1	-1	2	0	-1	1.633	0^0	-0.577	$\sqrt{3}$	109.46^0
$\vec{V}_2$	1	1	-1	1	2	1	1.633	60^0	0.577	$\sqrt{3}$	70.54^0
$\vec{V}_3$	-1	1	-1	-1	2	-1	1.633	120^0	-0.577	$\sqrt{3}$	109.46^0
$\vec{V}_4$	-1	1	1	-2	0	1	1.633	180^0	0.577	$\sqrt{3}$	70.54^0
$\vec{V}_5$	-1	-1	1	-1	-2	-1	1.633	240^0	-0.577	$\sqrt{3}$	109.46^0
$\vec{V}_6$	1	-1	1	1	-2	1	1.633	300^0	0.577	$\sqrt{3}$	70.54^0

Tables II–V are representing all the parameters in 3-D coordinates for zero vectors, small vectors, medium vectors, and large vectors, respectively.

In Fig. 9, three-level voltage vector's allocation in 3-D aspect $\{\vec{n}_\alpha, \vec{n}_\beta, \vec{n}_0\}$ is shown. In fact, when the zero-axis $\vec{n}_0$ is considered, there are seven voltage levels or units in zero-axis such as $\{-3, -2, -1, 0, 1, 2, 3\}$. In two positive units of zero-axis, $\vec{n}_0$, small vectors $\{\vec{V}_{02p}, \vec{V}_{04p}, \vec{V}_{06p}\}$ are allocated on this level. On the other hand, the combinations of small vectors and large vectors $\{\vec{V}_{01p}, \vec{V}_2, \vec{V}_{03p}, \vec{V}_4, \vec{V}_{05p}, \vec{V}_6\}$ are allocated to one positive unit of the zero-axis shown in Fig. 10. All the Medium vectors $\{\vec{V}_{12}, \vec{V}_{23}, \vec{V}_{34}, \vec{V}_{45}, \vec{V}_{56}, \vec{V}_{61}\}$ are allocated to the zero unit of the zero-axis or α–β horizontal

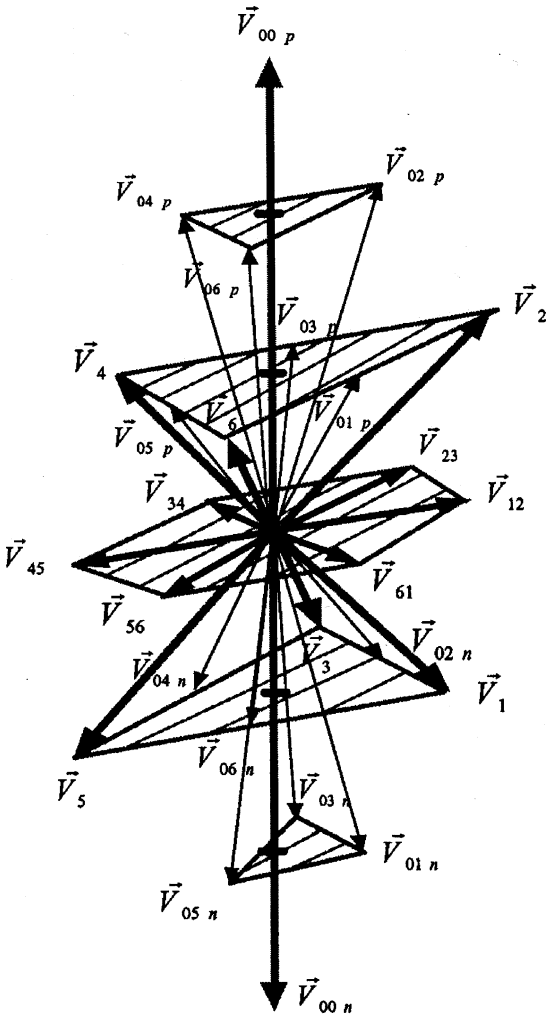

Fig. 9. Three-level voltage vector's allocation in 3-D aspect.

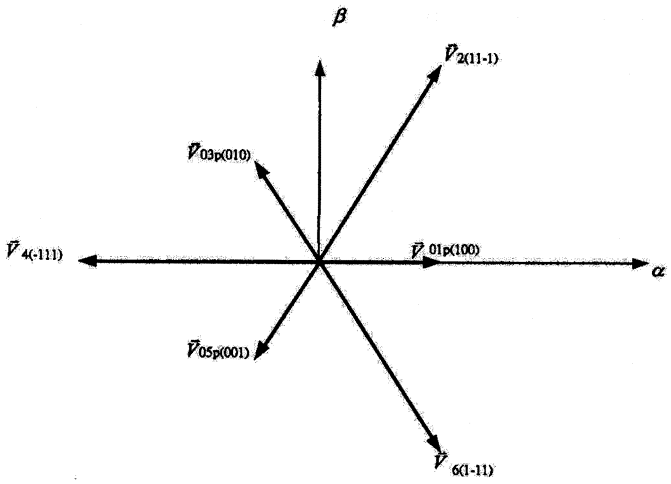

Fig. 10. Top view of vectors $\{\vec{V}_{01p}, \vec{V}_2, \vec{V}_{03p}, \vec{V}_4, \vec{V}_{05p}, \vec{V}_6\}$ in one positive unit zero-axis level.

plane. Vice versa, the vectors $\{\vec{V}_1, \vec{V}_{02n}, \vec{V}_3, \vec{V}_{04n}, \vec{V}_5, \vec{V}_{06n}\}$ and $\{\vec{V}_{01n}, \vec{V}_{03n}, \vec{V}_{05n}\}$ are allocated to negative unit's levels of zero-axis, respectively. It is noticed that their amplitudes, $r \in \{0, 0.816, 1.414, 1.633\}$, have different values.

III. Control Strategy

A. Fixed Switching Voltage Control Signal

The basic concept of power quality compensator is to inject the same negative amplitude of current harmonics, reactive and unbalanced currents into the system so that the generator can give only balance sinusoidal current to the load in order to optimize the power flow capacity. The compensated current will be focused in this section in order to obtain the corresponding voltage space vector for the PWM pattern's generation. To consider the injected current vector $\vec{i}_c$, that can be composed of $\{i_{ca}, i_{cb}, i_{cc}\}$ or $\{i_{c\alpha}, i_{c\beta}, i_{c0}\}$, into the system, only the coupling terminal voltage $\vec{v}_s$, $\{v_{Sa}, v_{Sb}, v_{Sc}\}$ or $\{v_{S\alpha}, v_{S\beta}, v_{S0}\}$, and the shunt balanced connected three-phase four-wired converter are studied. According to the instantaneous α–β–0 transformation's concept and referred to Fig. 2, the equivalent instantaneous voltage vector can be expressed as (14) and it is equivalent to (9). The voltage vector $\vec{v}$, that is the output terminal voltage of the 3-level inverter, should be generated according to the 3DPWM concept, the required current vector $\vec{i}_c$ and the coupling terminal voltage vector $\vec{v}_s$

$$\vec{v} = -R_c\vec{i}_c - L_c\frac{d\vec{i}_c}{dt} + \vec{v}_S. \tag{14}$$

Solving the equation (14) and assuming the sampling instants between KT and $(K+1)T$, the discrete compensated current can be expressed as

$$\begin{aligned}\vec{i}_c[(K+1)T] = {} & e^{-(R_c/L_c)T}\cdot\vec{i}_c[KT] \\ & + \int_{KT}^{(K+1)T} e^{-(R_c/L_c)[(K+1)T-t']}\,dt' \\ & \cdot\frac{1}{L_c}\left(\vec{v}_S[KT] - \vec{v}[KT]\right).\end{aligned} \tag{15}$$

Furthermore

$$\begin{aligned}\vec{i}_c[(K+1)T] = {} & e^{-(R_c/L_c)T}\cdot\vec{i}_c[KT] \\ & + \frac{\vec{v}_S[KT] - \vec{v}[KT]}{R_c}\left(1 - e^{-(R_c/L_c)T}\right).\end{aligned} \tag{16}$$

The measured parameters are $\vec{i}_c[KT]$ and $\vec{v}_S[KT]$, where $\vec{i}_c[KT]$ is the compensated current from inverter at the time K and $\vec{v}_S[KT]$ is coupling terminal's voltage with the shunt connected three-phase four-wired three-level converter. The sampling period is already fixed with the value of T. The next expected compensated current from Inverter should be $\vec{i}_c[(K+1)T]$ which can be described as the required compensated error current vector (17), $\Delta\vec{i}[KT]$

$$\Delta\vec{i}[KT] = \vec{i}_c[(K+1)T]. \tag{17}$$

The current vector $\Delta\vec{i}[KT]$ can represent the required current that can compensate the harmonics, reactive and unbalanced current as well as the neutral line current. The next expected current $\vec{i}_c[(K+1)T]$ from the three-level inverter should be equaled to the required error current vector $\Delta\vec{i}[KT]$ in order to compensate the harmonics, reactive, unbalanced and neutral line currents. The current tracking error is given in equation (18), where C can be a large positive real number that can form a feedback loop to track the error between the required line current and the reference line current

$$\begin{aligned}\Delta\vec{i}[KT] = {} & \left(\vec{i}_{\alpha\beta0}^{\,Reference}[KT] - \vec{i}_{\alpha\beta0}^{\,load}[KT]\right) \\ & + C\left(\vec{i}_{\alpha\beta0}^{\,Reference}[KT] - \vec{i}_{\alpha\beta0}^{\,line}[KT]\right).\end{aligned} \tag{18}$$

The difference between the current reference and the actual load current would be the signal to compare with the injected current signal. The $i_{\alpha\beta0}^{Reference}[KT]$ is the reference signal that can be obtained by instantaneous reactive power compensation technique [13], [14] and the $i_{\alpha\beta0}^{load}[KT]$ is the actual load current that may be distorted by nonlinear load. It is because T is the fixed sampling period and the balanced coupling resistors, R_c and inductors, L_c are employed. Under the consideration of (16), the decay exponential function can be considered to be linear within a very short sampling time, T. Taking the rate of change of the exponential function with negative slope, the decay value in every sampling T can be obtained in

$$\Delta X = \frac{R_c}{L_c}\cdot e^{-(R_c/L_c)T}\cdot T. \tag{19}$$

$\vec{v}[KT]$ voltage vector can be obtained (20) with (16)–(19). The (20) needs to measure the coupling terminal voltage $\vec{v}_S[KT]$ and inverter current $\vec{i}_c[KT]$ at time KT with the required tracking current error $\Delta\vec{i}[KT]$. The voltage signal $\vec{v}[KT]$ should be the required voltage vector from the output terminal of three-level inverter in order to track the current error

$$\vec{v}[KT] = \frac{R_c}{\Delta X}\left\{\Delta\vec{i}[KT] - (1-\Delta X)\vec{i}_c[KT]\right\} + \vec{v}_S[KT]. \tag{20}$$

B. Cylindrical Coordinated 3DPWM Control Strategy in Three-Level Converter

1) Control Block Diagram: From the above section, the required compensating voltage signal $\vec{v}[KT]$ can be determined uniquely according to the measured parameters and the tracking current error. The $\vec{v}[KT]$ can be expressed in (9) by the Basis $\{\vec{n}_\alpha, \vec{n}_\beta, \vec{n}_0\}$ in 3D PWM voltage vector. However, cylindrical coordinate can represent any point in 3-D aspect $\{r, \theta, Z_0\}$. Under the consideration of the 3DPWM, the cylindrical coordinate control strategy is proposed. Fig. 11 shows the basic control block diagram of cylindrical coordinate 3DPWM technique. The terminal voltage, injected current from the inverter, the load current, the line current and the reference current should be received and sampled. The fixed switching voltage control vector can be calculated according to (18)–(20) from the sampled data, v_S, i_c, i_{Load}, i_{Line} and $i_{Reference}$. The required voltage vector $\vec{v}$ can be expressed by Cylindrical Coordinate in terms of r, θ and Z_0. According to the parameters, r, θ, and Z_0, switching tables can be defined and the triggered pulses, S_a, S_b, S_c, can be received. The following section will describe the logic design of the switching tables.

2) Switching Tables: Although the voltage vector $\vec{v}[KT]$ (20) can be determined, there is still limited number of

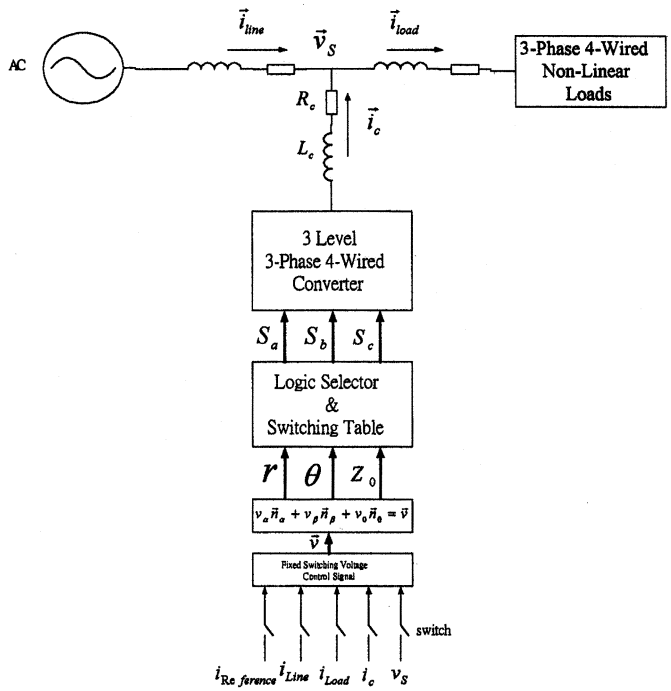

Fig. 11. Cylindrical control block diagram.

voltage vectors that can be supplied by three-level inverters. The switching tables can be designed according to the voltage vector $\vec{v}[KT]$; the Cylindrical Coordinate parameters $\{r, \theta, Z_0\}$ can be used to represent the voltage vector. There are four cases of switching tables that can be classified according to the polar voltage value, v_r: very small voltage, small voltage, medium voltage, and large voltage. The polar voltage value, v_r, is defined on the α–β plane. The switching tables can be determined according to the nearest voltage vector in 4 different cases. Under a certain polar voltage case, the nearest polar voltage vector that can be supplied by three-level converter is chosen to track the current error represented by $\vec{v}[KT]$ (20). It is assumed that all the discussion below will be considered in the normalized case: $V_{dc1} = V_{dc2} = 1$. There are four levels in the amplitude of $r \in \{0, 0.816, 1.414, 1.633\}$ in three-level inverters. Referring to the Fig. 3, the r and Z_0 has the same physical meaning as the polar voltage v_r and zero voltage v_0, respectively. Equations (21) and (22) are the polar voltage value v_r and polar angle θ_r, respectively

$$v_r = \sqrt{v_\alpha^2 + v_\beta^2} \tag{21}$$

$$\theta_r = \tan^{-1}\left(\frac{v_\beta}{v_\alpha}\right). \tag{22}$$

Case 1: Very Small Polar Voltage, v_r: According to Tables II–V, it is found that there are seven units or levels in zero-axis, such that $Z_0 \in \{-1.732, -1.155, -0.577, 0, 0.577\ 1.155, 1.732\}$. Although there are 7 zero-axis levels, the polar voltage is very small so that it is not needed to compensate the α and β components. Due to the vector choosing concept of the nearest polar voltage vector in this very small polar voltage case, the zero voltage compensation is under consideration only in this case. When the normalized polar voltage is within $v_r \in \{0, 0.408\}$, the only zero voltage vectors are activated. The zero voltage vectors are $\vec{V}_{00p}$, $\vec{V}_{000}$ and $\vec{V}_{00n}$. If $v_0 \in \{-0.866, 0.866\}$, $\vec{V}_{000}$ is chosen. When $v_0 < -0.866\}$, $\vec{V}_{00n}$ is used. During $v_0 > 0.866, 1.732\}$, $\vec{V}_{00p}$ is activated. When the required polar voltage is very small within $\{0, 0.408\}$, no matter what the polar angle θ_r is, Table VI is chosen.

TABLE VI
VERY SMALL v_r—ZERO VECTORS

v_r ° }0,0.408¡	v_0 > /0.866	v_0 ° }/ 0.866,0.866¡	v_0 @ 0.866
Any s_r	$\vec{V}_{00n}$? [/1 /1 /1]	$\vec{V}_{000}$? [0 0 0]	$\vec{V}_{00p}$? [1 1 1]

TABLE VII
SMALL v_r—SMALL VECTORS

$v_r \in \{0.408, \ 1.115\}$	$v_0 \geq 0$	$v_0 < 0$
$\theta_r \in \{330^0, 30^0\}$	$\vec{V}_{01p} = [1 \ 0 \ 0]$	$\vec{V}_{01n} = [0 \ -1 \ -1]$
$\theta_r \in \{30^0, 90^0\}$	$\vec{V}_{02p} = [1 \ 1 \ 0]$	$\vec{V}_{02n} = [0 \ 0 \ -1]$
$\theta_r \in \{90^0, 150^0\}$	$\vec{V}_{03p} = [0 \ 1 \ 0]$	$\vec{V}_{03n} = [-1 \ 0 \ -1]$
$\theta_r \in \{150^0, 210^0\}$	$\vec{V}_{04p} = [0 \ 1 \ 1]$	$\vec{V}_{04n} = [-1 \ 0 \ 0]$
$\theta_r \in \{210^0, 270^0\}$	$\vec{V}_{05p} = [0 \ 0 \ 1]$	$\vec{V}_{05n} = [-1 \ -1 \ 0]$
$\theta_r \in \{270^0, 330^0\}$	$\vec{V}_{06p} = [1 \ 0 \ 1]$	$\vec{V}_{06n} = [0 \ -1 \ 0]$

Case 2: Small Polar Voltage, v_r: When $v_r \in \{0.408, 1.115\}$, the small polar voltage is defined. In this case, polar angle θ_r (22) and zero voltage v_0 will be the other factors affecting the selected vector. Referring to the Table III and Fig. 9, the vectors $\vec{V}_{01p}$, $\vec{V}_{02p}$, $\vec{V}_{03p}$, $\vec{V}_{04p}$, $\vec{V}_{05p}$ and $\vec{V}_{06p}$ are allocated to the positive zero axis although there are two different zero levels. For example, the vectors $\vec{V}_{02p}$, $\vec{V}_{04p}$ and $\vec{V}_{06p}$ are on the two positive units of zero axis and the vectors $\vec{V}_{01p}$, $\vec{V}_{03p}$ and $\vec{V}_{05p}$ are allocated on the 1 positive level of zero axis. For another case, there are vectors $\vec{V}_{01n}$, $\vec{V}_{02n}$, $\vec{V}_{03n}$, $\vec{V}_{04n}$, $\vec{V}_{05n}$, $\vec{V}_{06n}$ that are allocated to the negative zero axis. The vectors $\{\vec{V}_{01n}, \vec{V}_{03n}, \vec{V}_{05n}\}$ and $\{\vec{V}_{02n}, \vec{V}_{04n}, \vec{V}_{06n}\}$ are settled on the two negative units and one negative level of zero axis, respectively. There are two groups of vectors according to the positive and negative zero voltage v_0. In this small polar voltage case, the nearest polar voltage vector is chosen so that when the polar voltage of $\vec{v}[KT]$ is within $\theta_r \in \{330°, 30°\}$ then $\vec{V}_{01p}$ and $\vec{V}_{01n}$ can be chosen. However, if the zero voltage v_0 is positive, $\vec{V}_{01p}$ can be activated. Otherwise, $\vec{V}_{01n}$ can be chosen. For example, when $v_r = 0.5$, $\theta_r = 78°$ and $v_0 = 0.8$, the $\vec{V}_{02p}$ is chosen. According to the above consideration, Table VII can be defined.

Case 3: Medium Polar Voltage, v_r: When $v_r \in \{1.115, 1.524\}$, the required polar voltage is not small or large so that the medium polar voltage vectors are chosen. From Fig. 9, it is noticed that the medium voltage vectors are allocated on the zero voltage level. The medium polar vectors $\{\vec{V}_{12}, \vec{V}_{23}, \vec{V}_{34}, \vec{V}_{45}, \vec{V}_{56}, \vec{V}_{61}\}$ are laid on the α–β plane. The medium polar voltage vectors don't have the compensating action in zero-axis. However, the nearest polar voltage vector will be chosen according to

TABLE VIII
MEDIUM v_r—MEDIUM AND ZERO VECTORS

$v_r \in \{1.115,\ 1.524\}$	$v_0 < -0.289$	$-0.289 \le v_0 \le 0.289$	$v_0 > 0.289$
$\theta_r \in \{0^0, 60^0\}$	$\vec{V}_{00n} = [-1\ -1\ -1]$	$\vec{V}_{12} = [1\ 0\ -1]$	$\vec{V}_{00p} = [1\ 1\ 1]$
$\theta_r \in \{60^0, 120^0\}$	$\vec{V}_{00n} = [-1\ -1\ -1]$	$\vec{V}_{23} = [0\ 1\ -1]$	$\vec{V}_{00p} = [1\ 1\ 1]$
$\theta_r \in \{120^0, 180^0\}$	$\vec{V}_{00n} = [-1\ -1\ -1]$	$\vec{V}_{34} = [-1\ 1\ 0]$	$\vec{V}_{00p} = [1\ 1\ 1]$
$\theta_r \in \{180^0, 240^0\}$	$\vec{V}_{00n} = [-1\ -1\ -1]$	$\vec{V}_{45} = [-1\ 0\ 1]$	$\vec{V}_{00p} = [1\ 1\ 1]$
$\theta_r \in \{240^0, 300^0\}$	$\vec{V}_{00n} = [-1\ -1\ -1]$	$\vec{V}_{56} = [0\ -1\ 1]$	$\vec{V}_{00p} = [1\ 1\ 1]$
$\theta_r \in \{300^0, 360^0\}$	$\vec{V}_{00n} = [-1\ -1\ -1]$	$\vec{V}_{61} = [1\ -1\ 0]$	$\vec{V}_{00p} = [1\ 1\ 1]$

TABLE IX
LARGE v_r—LARGE AND SMALL VECTORS

$v_r > 1.524$	$v_0 \ge 0$	$v_0 < 0$
$\theta_r \in \{330^0, 30^0\}$	$\vec{V}_{01p} = [1\ 0\ 0]$	$\vec{V}_1 = [1\ -1\ -1]$
$\theta_r \in \{30^0, 90^0\}$	$\vec{V}_2 = [1\ 1\ -1]$	$\vec{V}_{02n} = [0\ 0\ -1]$
$\theta_r \in \{90^0, 150^0\}$	$\vec{V}_{03p} = [0\ 1\ 0]$	$\vec{V}_3 = [-1\ 1\ -1]$
$\theta_r \in \{150^0, 210^0\}$	$\vec{V}_4 = [-1\ 1\ 1]$	$\vec{V}_{04n} = [-1\ 0\ 0]$
$\theta_r \in \{210^0, 270^0\}$	$\vec{V}_{05p} = [0\ 0\ 1]$	$\vec{V}_5 = [-1\ -1\ 1]$
$\theta_r \in \{270^0, 330^0\}$	$\vec{V}_6 = [1\ -1\ 1]$	$\vec{V}_{06n} = [0\ -1\ 0]$

the required voltage signal $\vec{v}[KT]$ (20). When the zero voltage value is not too large, $v_0 \in \{-0.289, 0.289\}$, the medium polar voltage vectors can be chosen and they can be uniquely defined according to the same consideration in case 2 and their polar angle θ_r, shown in the middle column of the Table VIII. However, when the zero voltage value needs to be large, the zero voltage vectors are chosen. The zero voltage error is forced to be reduced first and reaches to a small value, e.g., 0.289. Then, the medium voltage vectors are activated. According to the above logic, Table VIII is defined for medium required voltage.

Case 4: Large Polar Voltage, v_r: When $v_r > 1.524$, large polar voltage will be defined. In this case, large voltage and small voltage vectors are chosen. However, large voltage vectors should be chosen but there are limited numbers of large vectors that can be supplied in three-level inverters. Although, it needs large vectors, small voltage vectors can be chosen instead. It is already the nearest polar voltage vector that can be chosen in three-level case according to the required voltage $\vec{v}[KT]$. In Fig. 10, the positive large and small vectors $\{\vec{V}_{01p}, \vec{V}_2, \vec{V}_{03p}, \vec{V}_4, \vec{V}_{05p}, \vec{V}_6\}$ are shown. In the other case, the vectors $\{\vec{V}_1, \vec{V}_{02n}, \vec{V}_3, \vec{V}_{04n}, \vec{V}_5, \vec{V}_{06n}\}$ laid in the negative zero region. According to the discussion in Case 2, the nearest polar vector is chosen. When the $\vec{v}[KT]$ is detected, the normalized polar voltage $v_r > 1.524$, zero voltage $v_0 \ge 0$ and polar angle θ_r is within 330° and 30°, the nearest polar vector is chosen so that $\vec{V}_{01p}$ will be activated. For example, $\vec{v}[KT]$ can be represented by $v_r = 1.7$, $\theta_r = 78°$ and $v_0 = 0.8$, the $\vec{V}_2$ can be chosen. Table IX is defined for the large polar voltage.

From the above discussion, the polar voltage v_r, polar angle θ_r and zero voltage v_0 are the parameters to design the activated vector. Those three parameters are dedicated to represent a 3-D vector in cylindrical coordinate. As there are limited number of supplied voltage vectors by three-level inverter, the nearest polar vector is chosen according to the polar voltage, polar angle and zero voltage of $\vec{v}[KT]$ (20). It is clear that the number of states will be equaled to the available vectors provided by three-level inverters. In the conventional three-level PWM techniques, there are 19 states and 27 available vectors. However, in 3DPWM, there are 27 states that are equaled to the number of available vectors in three-level inverters.

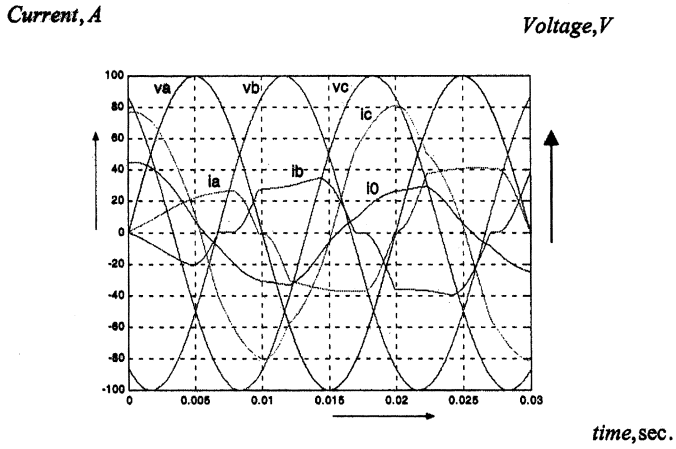

Fig. 12. Voltage and load current before compensation.

IV. SIMULATION RESULTS AND DISCUSSION

The simulation is performed by MATLAB as the power quality compensator with fixed switching frequency. The performance indices are proposed for 3DPWM and cylindrical coordinate control strategy is compared to fixed switching sign cubical control strategy [15].

A. Active Filter With Fixed Switching Frequency

A simulation test is performed by cylindrical coordinate control of 3-D pulse width modulation technique proposed in last section as a power quality compensator to compensate the harmonics, reactive and unbalance currents as well as the neutral line current in three-phase four-wired system. Fig. 12 shows the nonlinear load current and voltage waveforms before the compensation. Fig. 13 is the load current in α–β frame and Fig. 14 expresses the load current before the compensation in 3-D aspect.

Fig. 15 shows the waveforms after compensated by 10 KHz fixed switching cylindrical coordinate control strategy of 3-D PWM. It is obvious that this novel proposed control strategy in 3DPWM could reduce the harmonic spectrum and compensate the reactive and unbalance currents with eliminating neutral current as well. Figs. 16 and 17 show the current locus after compensation in 2-D and 3-D manners, respectively. It shows that center-split 3-arms inverters can compensate harmonics, reactive, unbalanced and neutral line currents by 3DPWM technique. The simulation results show its validity by cylindrical coordinate control of 3DPWM technique. The following section will compare the performance of sign cubical hysteresis control [15] and this proposed control strategy, "cylindrical coordinate control strategy."

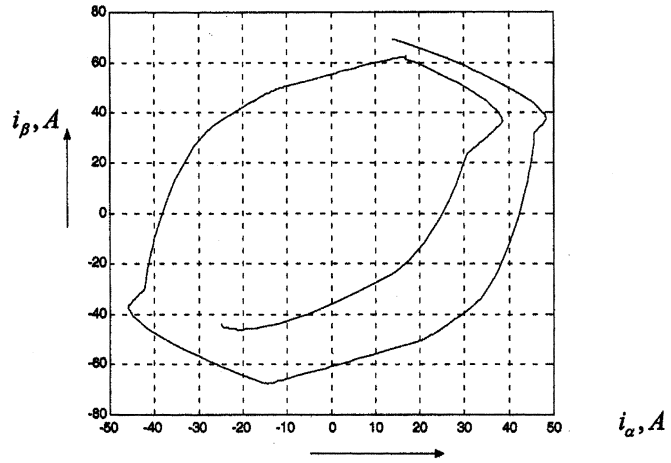

Fig. 13. Load current in α–β frame before compensation.

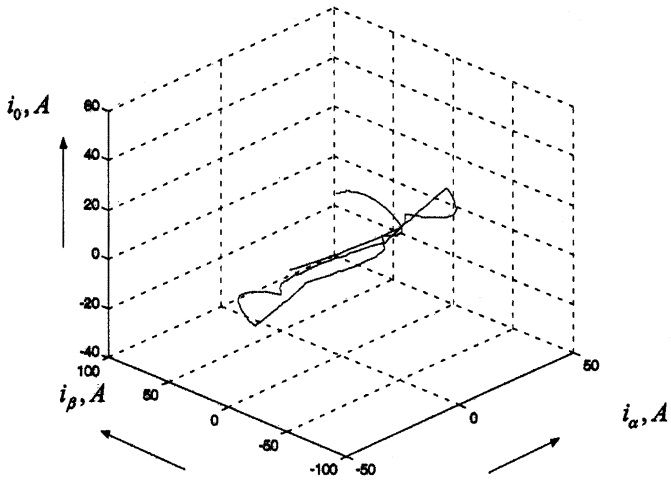

Fig. 14. Load current before compensation in 3-D, α–β–0 frame.

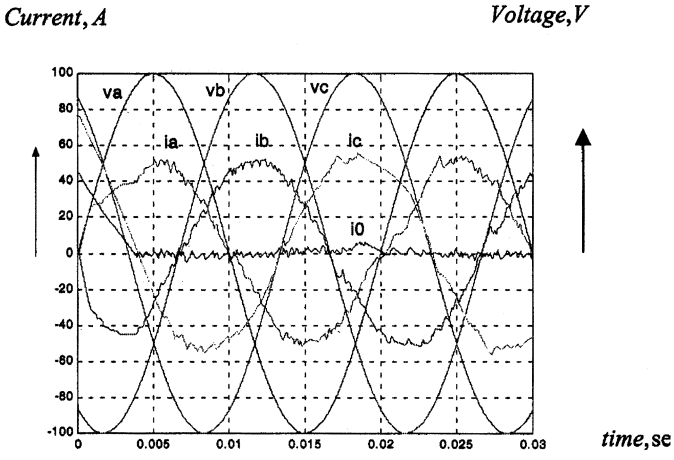

Fig. 15. Voltage and current waveforms after compensation by 10 KHz cylindrical coordinate control strategy.

B. Comparison With 3DPWM by Fixed Sign Cubical Hysteresis Control Strategy

1) Fixed Switching Sign Cubical Hysteresis Control Strategy [15]: In 3DPWM, there are three different hysteresis limits in three different α, β and 0 frames. If the hysteresis limits for $\Delta\alpha$, $\Delta\beta$ and $\Delta 0$ are equaled to each other ($\Delta\alpha = \Delta\beta = \Delta 0$), the cubical hysteresis control technique can be received. There are three levels $\{1, 0, -1\}$ in this sign cubical hysteresis control method and the sign of triggering pulses is an important parameter in tracking the current reference so as to choose the correct vectors. When the difference between the reference signal and actual input signal is larger than the Hysteresis limited value, it will trigger to positive or, vice versa, to negative one according to its direction. However, when the difference is less than the Hysteresis limit, there will be the zero level. According to the above logic consideration, there are three voltage levels in three switches so that there will be 27 states. Further consideration in those 27 states, there are the issues: vector-pairs and special vectors [15]. Tables X and XI show the vector-pairs and special vectors.

It is obvious that in the vector-pairs this sign cubical hysteresis control method will have two vectors in same direction

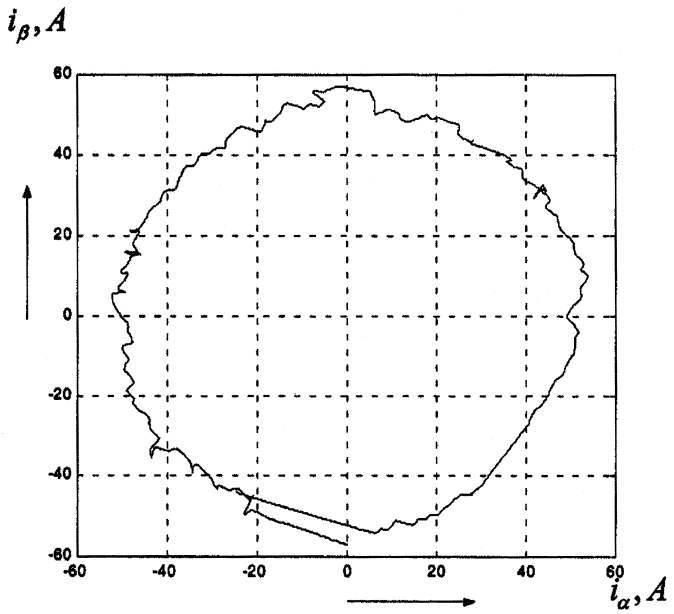

Fig. 16. Current locus after compensation in α–β frame by 10 KHz cylindrical coordinate control strategy.

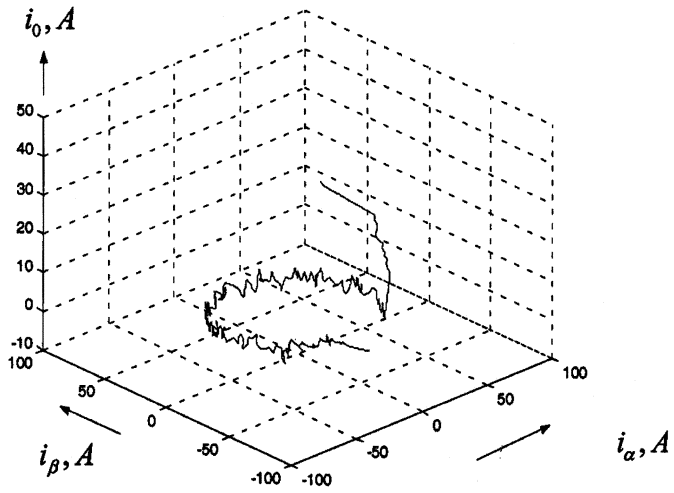

Fig. 17. Current locus after compensation in 3-D aspect by 10 KHz cylindrical coordinate control strategy.

TABLE X
VECTORS-PAIRS

	S_α	S_β	S_0	Large Vectors	Small Vectors
1	+	0	-	$\vec{V}_1$	$\vec{V}_{01n}$
2	+	+	+	$\vec{V}_2$	$\vec{V}_{02p}$
3	-	+	-	$\vec{V}_3$	$\vec{V}_{03n}$
4	-	0	+	$\vec{V}_4$	$\vec{V}_{04p}$
5	-	-	-	$\vec{V}_5$	$\vec{V}_{05n}$
6	+	-	+	$\vec{V}_6$	$\vec{V}_{06p}$

TABLE XI
SPECIAL VECTORS

	S_α	S_β	S_0	Possible Selection Vectors			
1	+	0	0	$\vec{V}_1$	$\vec{V}_{12}$	$\vec{V}_{01p}$	$\vec{V}_{01n}$
2	-	0	0	$\vec{V}_4$	$\vec{V}_{45}$	$\vec{V}_{04p}$	$\vec{V}_{04n}$
3	0	+	+	$\vec{V}_{23}$	$\vec{V}_{00p}$	$\vec{V}_{02p}$	$\vec{V}_{03p}$
4	0	+	-	$\vec{V}_{23}$	$\vec{V}_{00n}$	$\vec{V}_{02n}$	$\vec{V}_{03n}$
5	0	-	-	$\vec{V}_{56}$	$\vec{V}_{00n}$	$\vec{V}_{06n}$	$\vec{V}_{05n}$
6	0	-	+	$\vec{V}_{56}$	$\vec{V}_{00p}$	$\vec{V}_{06p}$	$\vec{V}_{05p}$

such as $\vec{V}_1$ and $\vec{V}_{01n}$, $\vec{V}_2$ and $\vec{V}_{02p}$, $\vec{V}_3$ and $\vec{V}_{03n}$, $\vec{V}_4$ and $\vec{V}_{04p}$, $\vec{V}_5$ and $\vec{V}_{05n}$, and, $\vec{V}_6$ and $\vec{V}_{06p}$. For the special vectors, there are many selections for compensation, four possible selective vectors are listed only. When the controller received the signals, e.g., $S_\alpha > 0$, $S_\beta = 0$ and $S_0 = 0$, a vector can be selected from $\vec{V}_1$, $\vec{V}_{12}$, $\vec{V}_{01p}$ or $\vec{V}_{01n}$. Those vectors ($\vec{V}_1$, $\vec{V}_{12}$, $\vec{V}_{01p}$ or $\vec{V}_{01n}$) can give different actions in α frame, β frame and 0 frame respectively. For example, the vectors $\vec{V}_{01p}$ and $\vec{V}_{01n}$ will give improvement in α frame, but they will force the increase of zero axis error in positive and negative directions respectively. When the switching frequency is randomly chosen, the switching frequency may be too large and it gets over the practical switching limits of IGBTs so that fixed cubical hysteresis control method is chosen. According to the above control strategy [15], the following conclusion can be drawn.

1) The compensated vector is not uniquely defined and it may enhance one improvement in one direction and intend a dedicated error in another direction.

2) When the switching frequency is fixed, there will be over-compensation or under-compensation so that the relative error will be increased.

3) Due to point 2) above, the compensated results may not be stable and the switching frequency should be very high in order to maintain the stable compensated results.

4) The performance of this system will be affected by the sampling rate, the inductance and resistance values of coupling transformer, voltage difference between the terminals of three-level inverter and the coupling point with the network and the values of the hysteresis limit.

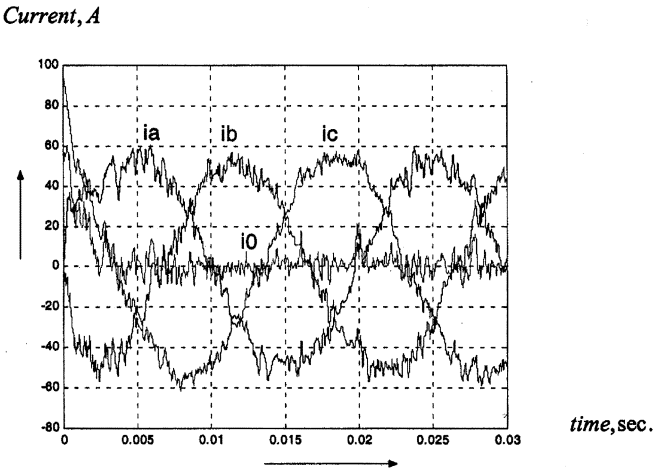

Fig. 18. Current waveforms after compensation by 20 KHz sign cubical control strategy.

5) According to the simulation results in this section, the switching frequency is relatively high so that the switching loss will be higher.

6) The controller will be simple and easy to be implemented.

2) Three-Dimensional Performance Indices: The performance indices are proposed in equations from (23)–(26) in order to compare the achievement between Proposed cylindrical coordinate control strategy and fixed switching sign cubical hysteresis control technique [15] in 3-D pulse width modulation of three-phase four-wired three-level inverter. The indices J_α, J_β and J_0 are the average absolute error in the α, β and 0 frames of one period. The index, $J_{\alpha\beta 0}$, is the sum of all absolute mean error. The objective is to reduce all the proposed indices as small as possible in all 3-D compensated techniques

$$J_\alpha = \frac{1}{T}\int_0^T |\Delta i_\alpha|\, dt \tag{23}$$

$$J_\beta = \frac{1}{T}\int_0^T |\Delta i_\beta|\, dt \tag{24}$$

$$J_0 = \frac{1}{T}\int_0^T |\Delta i_0|\, dt \tag{25}$$

$$J_{\alpha\beta 0} = \frac{1}{T}\int_0^T (|\Delta i_\alpha| + |\Delta i_\beta| + |\Delta i_0.|)\, dt. \tag{26}$$

Figs. 18–20 show the current waveforms after compensated by fixed switching sign cubical hysteresis control strategy in 3DPWM with 20 KHz switching frequency in time domain, 2-D α–β frame and 3-D α–β–0 frame, respectively. However, all the simulation results of the cylindrical coordinate control strategy are achieved by 10 KHz switching frequency.

Figs. 21 and 22 show the waveforms of Δi_α, Δi_β and Δi_0 by 20 KHz sign cubical control compensation and 10 KHz cylindrical coordinate control strategy, respectively. Table XII summarizes the values obtained by simulation according to the proposed performance indices and total harmonics distortion (THD) of compensated current waveforms in phase a, b and c. It is obvious that the compensated results are better by cylindrical coordinate control strategy. Although the switching frequency of sign cubical control strategy is double of the

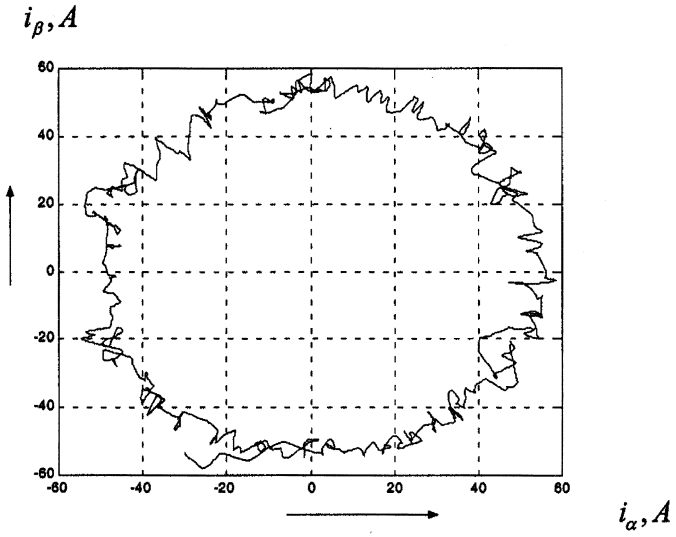

Fig. 19. Current locus after compensation in α–β frame by 20 KHz fixed switching sign cubical hysteresis control strategy.

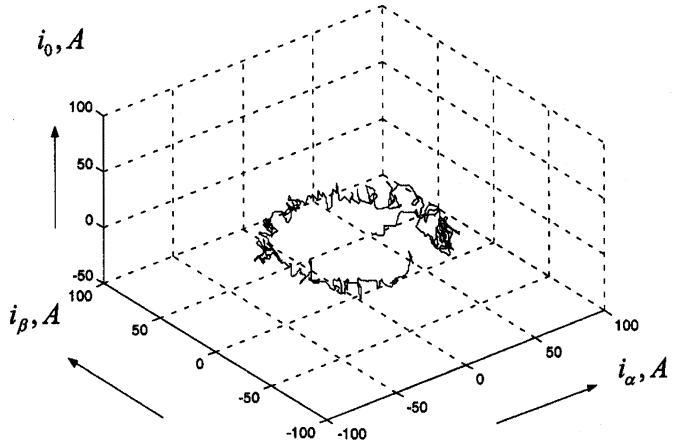

Fig. 20. Current locus after compensation in 3-D aspect by 20 KHz fixed switching sign cubical hysteresis control strategy.

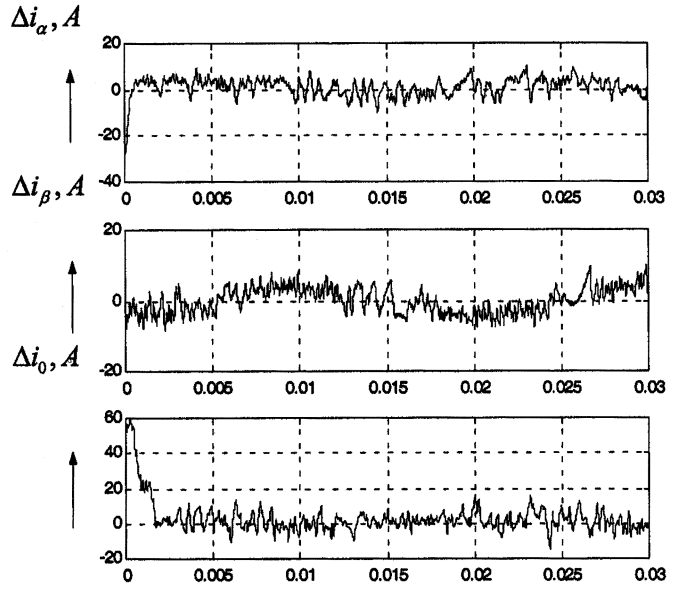

Fig. 21. Waveforms of Δi_α, Δi_β and Δi_0 by 20 KHz sign cubical control.

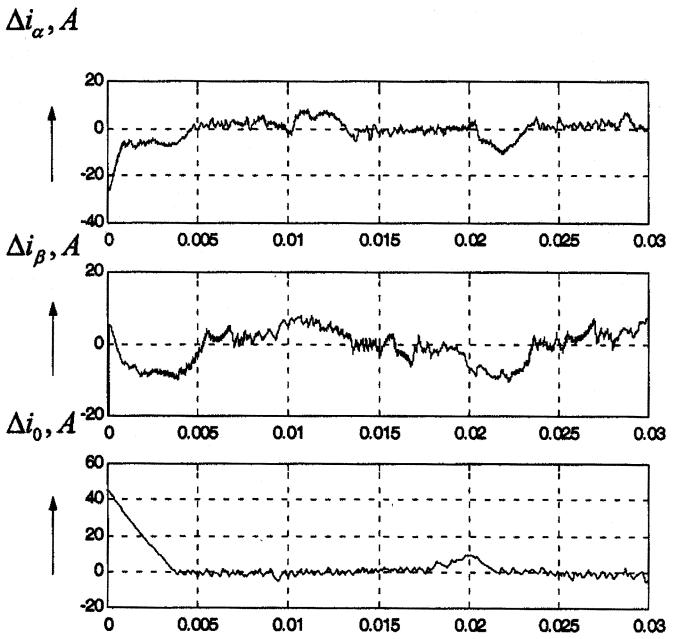

Fig. 22. Waveforms of Δi_α, Δi_β and Δi_0 by 10 KHz cylindrical coordinate control.

TABLE XII
COMPARISON OF 3 DIMENSIONAL PULSE WIDTH MODULATION TECHNIQUES

Comparison of 3 Dimensional Pulse Width Modulation Techniques	Without Compensation	Sign Cubical Control Strategy 20KHz	Cylindrical Coordinate Control Strategy 10K Hz
(%) THD of Phase a Current	30.47 %	11.82 %	7.17 %
(%) THD of Phase b Current	32.22 %	10.40%	5.72 %
(%) THD of Phase c Current	41.47 %	8.49 %	6.26 %
J_α	15.59	3.063	2.249
J_β	12.13	3.092	3.392
J_0	18.67	3.53	1.339
$J_{\alpha\beta 0}$	46.39	9.685	6.98

other, the performance indices of cylindrical coordinate control method are better and there is further improvement in zero-axis.

Comparing the THD values of the line currents, the performance of 10 KHz cylindrical coordinate control one is better than the 20 KHz sign cubical one by about 37% in average. On the other hand, there are around 79.12% and 84.95% improvement in the value of $J_{\alpha\beta 0}$ in the sign cubical control and cylindrical coordinate control, respectively. Checking the values of J_α, J_β and J_0, the compensated improvement is almost the same in α, β and 0 axes of Sign Cubical one. However, there is better improvement in the zero-axis of cylindrical coordinate control strategy.

3) Switching Losses: The IGBT Switching loss can be classified as turn-on and turn-off losses. Equation (27) is the total turn-on and turn-off power loss given in [18]. In equation (27), V_{CC}, I_{CM}, I_{CN}, t_{rN}, t_{fN} and f are the dc Bus Voltage, maximum collector current, rated collector current, rated rise time, rated fall time and switching frequency respectively. It will be obvious that the IGBT switching loss will be directly proportional to the switching frequency and the number of commutation

$$P_{loss} = V_{CC} I_{CM} f \left(\frac{1}{8} t_{rN} \frac{I_{CM}^2}{I_{CN}} + t_{fN} \left(\frac{1}{3\pi} + \frac{1}{24} \frac{I_{CM}}{I_{CN}} \right) \right). \quad (27)$$

From the above results, the switching frequency is chosen to be 20 KHz in fixed switching sign cubical hysteresis control technique, but the switching frequency is only 10 KHz in this proposed cylindrical coordinate control strategy. It is obvious that the switching loss in 10 KHz must be smaller. The proposed technique in this paper gives better performance with less switching loss.

V. Conclusion

The shunt-connected three-level converter in three-phase four-wired system is studied with consideration of the 3-D voltage vectors. Mathematical model of trilevel converter is addressed in a–b–c–0 frame. Detailed analysis of 3DPWM in two-level and three-level inverters is performed in rectangular, cylindrical and spherical coordinates. In conventional PWM techniques, the numbers of states in two-level and three-level systems are seven and 19, respectively. However, in 3DPWM, the number of states will be equaled to the number of available vectors. The fixed switching modified voltage control signal is received according to the required current vector. The switching tables can be defined according to the cylindrical coordinate parameters, $\{v_r, \theta_r, v_0\}$ and the four classification of polar voltage. Comparative study of 3-D three-level PWM with the control of fixed switching sign cubical hysteresis strategy and the proposed novel control technique "cylindrical coordinate control strategy" is achieved. The main drawbacks of the fixed switching sign cubical hysteresis control strategy are as follows.

1) "Special Vectors" that intends one improvement in one direction and increases dedicated error in another direction.
2) Switching frequency is relatively high so that it increases the switching loss.
3) The performance results can be affected by the sampling rates, the inductance and resistance values of coupling transformer, voltage difference between the terminals of three-level inverter and the coupling point with the network and the values of the Hysteresis limit, and it may cause unstable compensation: over-compensation or under-compensation.

However, the proposed cylindrical coordinate control strategy is accomplished without "special vectors" and the compensated vector can be uniquely defined such that better performance can be achieved. Its switching frequency is reduced with better improvement in reducing harmonics and neutral current as well. In addition to that, novel performance indices are proposed to match the 3-D PWM performance criteria. The results show that the proposed cylindrical coordinate control strategy overcomes the drawbacks of the fixed switching sign cubical hysteresis control due to the dedication of complex controller.

References

[1] L. M. Tolbert, F. Z. Peng, and T. G. Habetler, "Multilevel PWM methods at low modulation indices," *IEEE Trans. Power Electron.*, vol. 15, pp. 719–725, July 2000.

[2] S. Halasz, B. T. Huu, and A. Zakharov, "Two-phase modulation technique for three-level inverter-FED AC drives," *IEEE Trans. Power Electron.*, vol. 147, pp. 1200–1211, Dec. 2000.

[3] P. Enjeti and R. Jakkli, "Optimal power strategies for Neutral Point Clamped (NPC) inverter topology," *IEEE Trans. Ind. Applicat. Syst.*, pp. 924–930, Oct. 1989.

[4] H. L. Liu, G. H. Cho, and S. S. Park, "Optimal PWM design for high power three-level inverter through comparative studies," *IEEE Trans. Power Electron.*, vol. 10, pp. 38–47, Jan. 1995.

[5] J. K. Steinke, "Switching frequency optimal PWM control of a three-level inverter," *IEEE Trans. Power Electron.*, vol. 7, pp. 487–496, July 1992.

[6] B. Velaerts, P. Mathys, and G. Bingen, "New developments of 3-Level PWM strategies," in *Proc. EPE'89 Conf.*, Aachen, Germany, 1989, pp. 411–416.

[7] N. Celanovic and D. Boroyevich, "A fast space-vector modulation algorithm for multilevel three-phase converters," *IEEE Trans. Ind. Applicat.*, vol. 37, pp. 637–641, Mar./Apr. 2001.

[8] J. Holtz, "Pulsewidth modulation—A survey," *IEEE Trans. Ind. Electronics*, vol. 99, pp. 410–420, Dec. 1992.

[9] M. P. Kazmierkowski and M. A. Dzieniakowski, "Review of current regulation techniques for three-phase PWM inverters," in *Proc. IEEE IECON'9 Conf.*, Bologna, Italy, 1994, pp. 567–575.

[10] A. Trzynadlowski, "An overview of modern PWM techniques for three-phase, voltage-controlled, voltage–source inverters," in *Proc. IEEE ISIE'96 Conf.*, Warsaw, Poland, pp. 25–39.

[11] M. Aredes, J. Hafner, and K. Heumann, "Three-phase four-wire shunt active filter control strategies," *IEEE Trans. Power Electron.*, vol. 12, pp. 311–318, Mar. 1997.

[12] A. Dastfan, V. J. Gosbell, and D. Platt, "Control of a new active power filter using 3-D vector control," *IEEE Trans. Power Electron.*, vol. 15, pp. 5–12, Jan. 2000.

[13] H. Agaki, Y. Kanazawa, and A. Nabae, "Instantaneous reactive power compensators comprising switching devices without energy storage components," *IEEE Trans. Ind. Applicat.*, vol. IA-20, pp. 625–630, May/June 1984.

[14] F. Z. Peng, G. W. Ott, and D. J. Adams, "Harmonic and reactive power compensation based on the generalized instantaneous reactive power theory for three-phase four-wire systems," *IEEE Trans. Power Electron.*, vol. 13, pp. 1174–1181, Nov. 1998.

[15] M.-C. Wong, Z.-Y. Zhao, Y.-D. Han, and L.-B. Zhao, "Three-dimensional pulse-width modulation technique in three-level power inverters for three-phase four-wired system," *IEEE Trans. Power Electron.*, vol. 16, pp. 418–427, May 2001.

[16] O. Kukrer, "Discrete-time current control of voltage-fed three-phase PWM inverters," *IEEE Trans. Power Electron.*, vol. 11, pp. 260–269, Mar. 1996.

[17] R. Rojas, T. Ohnishi, and T. Suzuki, "An improved voltage vector control method for neutral-point-clamped inverter," *IEEE Trans. Power Electron.*, vol. 10, pp. 666–672, Nov. 1995.

[18] F. Casanellas, "Losses in PWM inverters using IGBTs," *Proc. Inst. Elect. Eng.*, vol. 141, pp. 235–239, Sept. 1994.

Man-Chung Wong was born in Hong Kong in 1969. He received the B.Sc. and M.Sc. degrees in electrical and electronics engineering from the University of Macau, in 1993 and 1997, respectively, and is currently pursuing the Ph.D. degree at Tsinghua University, Beijing, China.

He was a Teaching Assistant at the University of Macau, from 1993 to 1997. Since 1998, he has been a Lecturer in the Department of Electrical and Electronics Engineering, University of Macau. His research interests are FACTS and DFACTS, power quality, custom power and PWM.

Mr. Wong received the Young Scientist Award from the "Insituto Internacional De Macau" in 2000 and the Young Scholar Award from the University of Macau in 2001.

Jing Tang (S'02) was born in Nanjing, China, in 1977. She received the B.Sc. degree from Southeast University, China, in 2000, and is currently pursuing the M.S. degree in the Department of Electrical and Electronics Engineering, University of Macau.

Her current area of research is the 3-D PWM in the power electronics field.

Ying-Duo Han was born in Shenyang, Liaoning province, China, in 1938. He received the B.S. and M.S. degrees from the Electrical Engineering Department, Tsinghua University, Beijing, China, in 1962 and 1965, respectively, and the Ph.D. degree from Erlangen-Nuerenberg University, Germany.

He is a Professor in the Electrical Engineering Department, Tsinghua University, and he was the Vice-Chairman and Chairman of the Electrical Engineering Department, from 1986 to 1995. Since 1989, he has been the head of Power Electronics Research Center, Tsinghua University. He is a Visiting Professor at the University of Macau, China. He is also the Vice-Chairman of the Beijing Society of Electrical Engineering and Vice-Editor of the *Journal of Electric Power System and Automation*. He has published two books and more than 100 papers. He has been engaged for more than 30 years in education and research work on electric power systems and the automation field. In recent years, he has engaged in FACTS and DFACTS, intelligent control, regional stability control, new dynamic security estimation, and control based on GPS.

Dr. Han received four-State-level prizes, and six first and second ranked Province-level and Ministry-level prizes. He is a Member of Chinese Academy of Engineering.